Imperial College London
Department of Physics

Critical gravitational collapse in AdS spacetime

Shuting Li

Submitted in part fulfilment of the requirements for the degree of
Msc in Quantum fields and fundamental forces of Imperial College, September 2012

Abstract

Motivated by AdS/CFT conjecture, we discussed gravitational collapse in Anti-de Sitter space-time. We reviewed the theory and numerical work on the critical solutions of black hole threshold both in flat space and AdS, and see similar critical behaviour. We also looked at some latest work in [21] about non-critical black hole formation in d+1 dimensional ($d \geq 3$) AdS, and notice some interesting properties of AdS.

Acknowledgements

I would like to express my gratitude towards Dr. Wiseman for agreeing to supervise my dissertation project and for his kind advice and generous support throughout this project. I also would like to thank theoretical physics group for organizing such a good msc course and for offering me the opportunity to study the subjects I am interested in. I would further like to thank my parents for the continuous support, without which my studies would not have been possible.

Contents

List of Tables

List of Figures

Chapter 1

Introduction

1.1 Why study AdS collapse

There is risen interest in the study of anti de-sitter (AdS) black hole formation in different dimensions. This is oringinated from the discovery of 2+1 dimension AdS black hole solutions[1] and is very much due to the AdS/CFT conjecture[2]. AdS/CFT is known as the simplest examples of gauge/gravity duality, which is a correspondence of anti-de-Sitter spacetimes and conformal field theories[3]. The gauge/gravity duality is an equality between a gravity theory on a d+1 dimensional spacetime (with a d dimensional asymptotic boundary) and a quantum field theory in d spacetime dimensions. The gravity theories are string theories and the quantum field theories are gauge theories, so this connection is also called gauge-string duality. A lot of evidence by far shows that this 'AdS/CFT conjecture' is true. Because of the correspondence of the two theories, we can solve some comparatively complicated quantum field theories by looking at equivalent theories in AdS gravities, which can be much more straightforward.

1.2 AdS/CFT relation

In this section, we present a very bisic instruction of AdS/CFT relation without including much detail. This relation assumes that the theory in an asymptotically AdS spacetime is

equivalent to a local quantum field theory (which we will see is a conformal field theory) on the boundary[3]. Let us understand this by recalling some detail of AdS spacetime first. AdS spacetime is a simplest solution of Einstein equations with a negative cosmological constant $\Lambda < 0$. AdS_{d+1} is a Lorentzian manifold of d+1 dimensional hyperbolic space. It is an early example of non-Euclidean geometry. The metric of AdS spacetime can be written as:

$$ds^2_{AdS_{d+1}} = R^2[-(r^2+1)dt^2 + \frac{dr^2}{r^2+1} + r^2 d\Omega^2_{d-1}] \tag{1.1}$$

where R is the radius of curvature, and $r^2 d\Omega^2_{d-1}$ is the metric of a unit sphere, S^{d-1}.

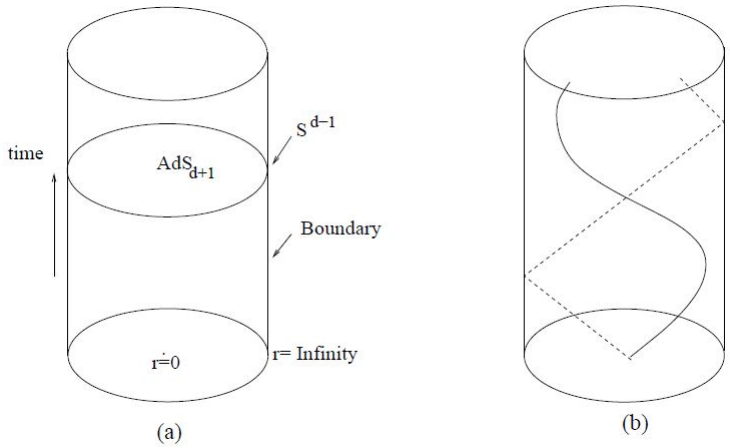

Figure 1.1: [3] (a) This solid cylinder is the *Penrosediagram* for AdS spacetime, where time axis is in the vertical direction. The boundary contains the time direction and a sphere, S^{d-1}, represented here as a circle. (b) Shows the geodesics : Massive geodesic (solid line) and a massless geodesic (dashed line).

We can see it looks like a flat space near $r = 0$, where $ds^2 \to R^2(-dt^2 + dr^2 + r^2 d\Omega^2)$. Note that as the radius r grow, $-g_{00}$ and the metric on the sphere also go larger. This gives a gravitational potential of $V \sim \sqrt{-g_{00}}$ to a slowly moving massive particle in the space, which attract it towards the origin. So if we put a particle at large enough r, it will move like a harmonic oscillator in r direction. This implies that if a massive particle has finite energy, it cannot escape to $r = \infty$. But a massless geodesic can go to infinity and return. In order to see this more clearly, we here introduce the *Penrose diagram*[1] of AdS. If we take a factor of $1 + r^2$ in the metric (1.1) and define $dx = \frac{dr}{1+r^2}$, we obtain a finite radial range. Then we get a solid

[1]Penrose diagram is "a two-dimensional diagram that captures the causal relations between different points in spacetime. Locally, the metric on a Penrose diagram is conformally equivalent to the actual metric in spacetime."

cylinder *Penrose diagram* with spatial boundary at $r = \infty$, which is finite in x coordinate, see Figure 1.1. The vertical direction is time and the side surface of the cylinder is the spherical metric, S^{d-1}. We can easily observe a symmetry of $R \times SO(d)$ of the metric in (1.1), but the total symmetries of AdS is known as SO(2, d). We can see such symmetries if we regard AdS as the hyperboloid in $R^{2,d}$ with the form of

$$-Z_{-1}^2 - Z_0^2 + Z_1^2 + \dots Z_d^2 = -R^2. \tag{1.2}$$

This is usful to recognize the symmetries, but we do not want to carry this too far, because the time direction t in 1.1, is compact but we want to see this time direction to be non-compact in most applications.

Because of such isometries of AdS, if we consider the oscillating trajectory of a massive particle, then we can 'boost' it to a frame where the particle is still. So the moving particle does not know that it is moving, which means AdS does not have a 'center'. We can always choose a 'center' by defining a lowest energy state of a particle.

We may carefully choose the coordinates(because they are not the full AdS) where the AdS metric is

$$ds^2 = R^2 \frac{-dt^2 + d\vec{x}_{d-1}^2 + dz^2}{z^2} \tag{1.3}$$

The boundary here is at $z = 0$. We may cut off half of the cylinder to get a wedge of $R \times S^{(d-1)}$. If we take the limit $t \to ix_0$ we obtain hyperbolic space. It is sometimes called the Euclidean AdS space. There is another isometry which rescales the coordinates $(t, \vec{x}, z) \to \lambda(t, \vec{x}, z)$. These coordinates only cover part of 1.1, but they are useful when we consider a CFT in Minkowski space, $R^{1,d-1}$.

We have mentioned the correspondence of an asymptotically AdS and a local quantum field theory on the boundary, $R \times S^{d-1}$. The action of the AdS isometries on the boundary is to map the points on it to points on a larger boundary. This is the action of a d dimensional conformal group, $SO(2, d)$. So we notice that the quantum field theory here is actually CFT. In fact, the rescaling symmetry of 1.3 can be thought as an expansion of the boundary. So the boundary theory is scale invariant. Scale invariant theories are often conformal invariant too;

in these theories the stress energy momentum tensor is traceless[3]. The traceless stress tensor gives that a field theory of metric $g^b_{\mu\nu}$ or $\omega^2(x)g^b_{\mu\nu}$ is basically the same. Due to the conformal symmetry, we can set the radius for the boundary, S^{d-1}, to one.

You may have noticed that we are talking about equivalence between bulk theories of defferent dimensions ($d+1$ dimensional with a d dimensional). There seem to be a contradiction when we count the degrees of freedom. We could understand this problem by considering entropy in the microcanonical ensemble at large energies. In a theory with massless fields, we expect the entropy to look like $S \sim \frac{V_{d-1}}{\beta_{d-1}}$. So for a boundary of CFT on $R \times S_3$ with $\beta \ll 1$(meaning large temperatures compared to the radius of S_3), we expect that the entropy to take the proportion

$$S \propto c\frac{1}{\beta_{d-1}}, \tag{1.4}$$

where c a dimensionless constant counting the effective number of fields. At the same time, if we consider from the bulk point of view, we seem to have another theory with massless particles: the gravitons. These gravitons are of larger entropy than the region of $r \sim 1$, where the volume has order one. Thus we get this relation in d spatial dimensions

$$S_{gas\,of\,gravitons} > \frac{1}{\beta^d} \tag{1.5}$$

For small enough β we see that 1.5 is bigger than 1.4. This appear to disagree with the assumption of AdS/CFT mentoned above. However, we have not yet taken the gravity in bulk theory into consideration. The gravity gives bounds to entropy, which is due to the emergence of black holes. The metric of AdS black holes is

$$ds^2_{AdS_{d+1}} = R^2(-(r^2+1-\frac{2gm}{r^{d-2}})dt^2 + \frac{dr^2}{r^2+1-\frac{2gm}{r^d-2}} + r^2 d\Omega^2_{d-1}) \tag{1.6}$$

where g is the ratio of Newton constant and AdS radius,

$$g \propto \frac{G_N^{d+1}}{R_{d-1}}. \tag{1.7}$$

The mass of the gas has the order of $m \sim \frac{1}{\beta_{d+1}}$, and the radius should be $r_z \sim \frac{1}{\beta}$. For $\beta \ll 1$ we can drop the 1 in 1.6 and obtain the Schwarschild radius of $r_s^d \sim gm \sim g/\beta^{d+1}$. For large enough temperatures, the Schwarschild radius is bigger than the size of the system, that is $1/\beta > 1/g$. Thus, 1.4 does not work for such large energies. In this case, we can compute the entropy from that of the black hole, which is $S_{BH} \sim \frac{1}{g}\frac{1}{d-1}$. The Hawing temperature for big black holes is $\beta \propto 1/r_s$. Note the entropy of the system goes larger as the horizon grows, $S \sim \frac{r_s^{d-1}}{g}$. Compare with 1.4, we have

$$c \propto \frac{1}{g} \propto \frac{R_{AdS}^{d-1}}{G_{N,d+1}}. \tag{1.8}$$

From above computation, we clarified the earlier questions. We see that AdS/CFT combines the entropy of a black hole with the original thermal entropy of a field theory. It displays the black hole as an ordinary thermal state in a quantum field theory. Also, it shows us a way to compute the thermal physics in quantum field theories with gravity dualities.

We want to be clear about the correspondence between states in AdS and states in the boundary it is neccessary to do the quantization of the corresponding field in AdS. We consider a simple example of an action in a massive scalar field in AdS spacetime

$$S = \int d^{d+1}x\sqrt{g}[(\nabla\phi)^2 + m^2\phi^2] \tag{1.9}$$

The computation carried out in [3] suggests that in position space this action is of the form

$$S = -\frac{2\nu\Gamma(\Delta)}{\pi^{\frac{d}{2}}\Gamma(\nu)} \int d^dx d^dy \frac{\phi_0(x)\phi_0(y)}{|x-y|^{2\Delta}} \tag{1.10}$$

The AdS/CFT dictionary states that this computation with fixed boundary conditions is related to "the generating function of correlation functions for the corresponding operator in the field theory" [29][30]. To look at such equality from quantum operator point, a field ϕ is related to

the single trace operator $\mathcal{O}$

$$Z_{Gravity}[\phi_0(x)] = Z_{FieldTheory}[\phi_0(x)] =< e^{\int d^d x \phi_0(x)\mathcal{O}(x)} > \tag{1.11}$$

We evaluate the leading approximation of the gravity side by e^{-S}. The correlation functions are then given by

$$< \mathcal{O}(x_1)\cdots\mathcal{O}(x_n) >= \frac{\delta}{\delta\phi_0(x_1)}\cdots\frac{\delta}{\delta\phi_0(x_n)} Z_{Gravity}[\phi_0(x)] \tag{1.12}$$

The correlation function can be broken into algebraic product of two point functions. The quadratic approximation of gravity answer is 1.10. If we include interactions in the bulk, we can compute the leading approximation by looking at the classical, non-linear solution with such boundary conditions and calculating the corresponding action. We can also evaluate the Feynman-Witten diagrams in the bulk [30] for perturbative computation.

Chapter 2

Critical phenomena in flat space gravititional collapse

2.1 Overview

In this chapter, we will generally understand the subject of critical collapse in flat space by studying the phenomena at the black hole threshold in the example of 3+1-dimensional general relativity. This chapter does not involve Ads spacetime.

The critical behaviour near the black hole threshold was discovered by Choptuik in numerical simulations of a spherical scalar field[4]. The black hole threshold solution has very simple and special structure. The black hole mass scaling and scale echoing give rise to the term "critical phenomena", which are described by exact solutions of the black hole threshold. To be specific, these phenomena can be explained in the following way.

We may take any one parameter p to represent the generic initial data in general relativity. If we tune the value of p carefully towards the black hole threshold, and compare the resulting spacetime solution as a function of p, in many situations, we observe the following criticle phenomena:

- Near the threshold, black holes with arbitarily small masses can be created, and the black hole has mass scale of

$$M \propto (p - p_*)^\gamma \tag{2.1}$$

where p is the initial data and black holes form for $p > p*$.

- With respect to the initial data we have, the *criticalexponent*γ is universal and depends only on the type of the collapsing matter. It is independent of the particular 1-parameter family.

- Before black hole formation, the spacetime approaches the *critical solution* in the region of large curvature. This solution is self-similar and also universal.

Such phenomena have been found in many other numerical and analytical studies in spherical symmetry, and a few have been seen in the collapse of axisymmetric gravitational waves in vacuum[5]. It is still unclear how the matter types can affect the critical phenomena in gravitational collapse.

In the simplest example of a dynamical system, a critical solution can be seen as an attracting fixed point on a surface that divides 2 basins of attraction in phase space. It is called the 'critical surface. This fixed point can be either a steady spacetime, or a scale-invariant and self-similar spacetime. The latter is relevant to the critical phenomena described above (Type II).

So we can study the field of critical phenomena in gravitational collapse by looking at the boundaries of different end states, such as black hole formation or dispersion. By fine-tuning initial p to the black hole threshold, these self-similar critical solutions provide a way of getting large spacetime curvature outside a black hole, and inside a naked singularity. Such solutions are likely to be useful in cosmology and quantum gravity.

2.2 Critical collapse

In this section we describe the basic theory underlying critical collapse of the type that forms arbitrarily small black holes (later called type II, also see Section 2.2.2 for type I).

The mathematical sources of its three main features that mentioned in the overview are covered:

- universality with respect to initial data
- black hole mass scaling
- scale-invariance of the critical solution

2.2.1 Universality

We can see GR as an infinite-dimensional continuous dynamical system and the points in the phase space are initial data sets which obey the Einstein constraints. If we choose a suitable gauge for the Einstein equations, the solution curves of the dynamical system are the spacetimes obeying the Einstein-matter equations, sliced by specific Cauchy surfaces of constant time t. An isolated system in GR can end up in two possible stable end states: "the formation of a single black hole in a collapse, or complete dispersion of the mass-energy to infinity" [31]. For a massless scalar field in spherical symmetry, these are the only possible end states (see Section 2.3). A point in phase space can always be classified as ending up in one of the two types of end state. In the simplest examples, the entire phase space splits into two halves, separated by a "critical surface".

By definition, a phase space trajectory that starts on a critical surface will never leave it. A critical surface is therefore a fully independent dynamical system with $d-1$ dimension if the full system is d dimensional. We consider there is an attracting fixed point, namely a 'critical point'. Then the critical surface is its attracting manifold, and the point is an attractor with codimension one in the system. This fact is visible in its linear perturbations: "It has an infinite number of decaying perturbation modes spanning the tangent plane to the critical surface, and a single growing mode not tangential to it" [31].

As illustrated in Figure 2.1, near the critical surface (but not necessarily near the critical point), any trajectory moves towards the critical point in a path nearly parallel to the critical surface. The process slows down near the critical point, and eventually moves away into the direction of growing mode. This is the origin of universality. The initial data does not contribute here,

except for the starting distance from the black hole threshold. When the initial phase point is closer to the 'critical surface', the solution curve will go closer to the critical point too. It will also stay close to the point for a longer time.

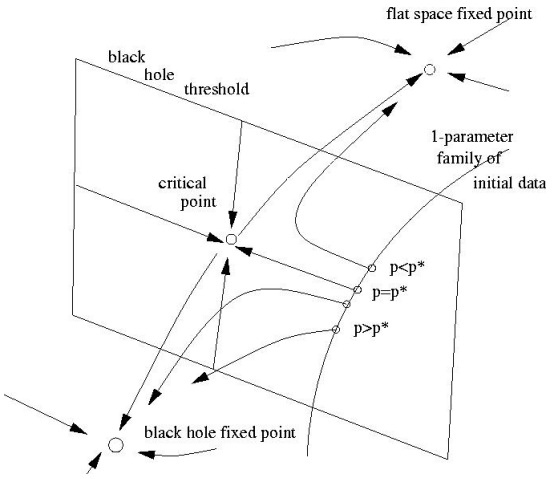

Figure 2.1: [31] This is the phase space picture for the black hole threshold of a continuously self-similar (CSS) solution. The arrow lines are time evolutions and the line without an arrow is not. The threshold is also presented by a 1-parameter family of initial data at $p = p_*$.

2.2.2 Type I and II

We focus on Type II critical phenomena throughout the chapter. To avoid any confusion, however, we want to be clear about what Type I is, and their differences. In type I critical phenomena, the same phase space picture as in Section 2.2.1 applies, but the critical solution is now steady or periodic with time, instead of self-similar or periodic in scale. It also has a finite mass and can be thought of as a "metastable star". (In statistical mechanics, Type I and II were named after first and second order phase transitions, where the order parameter is continuous and discontinuous, respectively.) Universality here implies that the black hole mass near the threshold is independent of the initial data. The scaling dimensionful quantity is not the black hole mass. The lifetime t_p of the intermediate state is

$$t_p = -\frac{1}{\lambda_0} ln\,|p - p_*| + constant \tag{2.2}$$

When a mass scale in the field equations becomes 'dynamically relevant', we see Type I critical

phenomena. (This mass scale might not set the mass of the critical solution to be absolute. There could be a set of critical solutions with respect to the initial conditions.) On the other hand, type II phenomena occur when the field equations do not contain a scale, or this scale is 'dynamically irrelevant'. This is due to the scale-invariance of the type II power law. In many systems, such as a massive scalar field, there are both type I and type II critical phenomena, depending on different regions of the initial data [6].

2.2.3 Black hole mass scaling

We present the computation of the critical exponent γ by considering the linear perturbations of critical solution. The calculation was proposed by Evans and Coleman [7] and done by Koike, Hara and Adachi [8] and Maison [9].

We take $Z(x)$ to be a set of scale-invariant variables, such as $\tilde{g}_{\mu\nu}$ and correspondently rescaled the matter variables. If we have is scale-invariant dynamics, $Z(x)$ is then an factor of the phase space of overall scale, with a solution $Z(x,\tau)$. We find that $Z(x)$ is a scale initial data of one parameter, while the overall scale is determined by τ.

Here we assume the critical solution is CSS for simplicity. The solution can be written as $Z(x,\tau) = Z_*(x)$. The linear perturbations of $Zx,\tau)$ depend only on the exponent of τ and a complex λ. It can be written as

$$\delta Z(x,\tau) = \sum_{i=1}^{\infty} C_i e^{\lambda_i \tau} Z_i(x) \tag{2.3}$$

where C_i are free constants. In the echoing region, the linear order of the solution is

$$Z(x.\tau;p) \simeq Z_*(x) + \sum_{i=1}^{\infty} C_i(p) e^{\lambda_i \tau} Z_i(x) \tag{2.4}$$

C_i depend on p in a complicated way. If Z_* is a critical solution, there is exactly one λ_i that has a positive real part [1], λ_0. As $\tau \to \infty$ and $t \to t_*$, all other perturbations vanish. We will retain only the one growing perturbation when considering this limit. The critical solution

[1] in fact it is purely real

corresponds to $p = p_*$ by definition, so we there must be $C_0(p_*) = 0$. Linearizing around p_*, we get

$$\lim_{\tau\to\infty} Z(x,\tau) \simeq Z_*(x) + \frac{dC_0}{dp}(p-p_*)e^{\lambda_0\tau}Z_0(x) \tag{2.5}$$

In this approximate form we can see the universality of solution Z_*. This also explains why we see more of the universal solutions as p is closer to p_*. There is a possible confusion here: because the critical solution is self-similar, it is not asymptotically flat. However, it can be "the limiting case of a family of asymptotically flat solutions in a region up to finite radius"[30]. It can be matched to an asymptotically flat solution at large radius, which is not universal.
In a range of τ, the approximate form of the solution is 2.5. We want to extract the Cauchy data at the value of $\tau = \tau_*$ in the range. It is defined by

$$\frac{dC_0}{dp}(p-p_*)e^{-\lambda_0\tau} \equiv \epsilon, \tag{2.6}$$

where $\epsilon \ll 1$ is a constant. This shows the linear approximation is still applied at this τ. We know that τ_* depends on p. At large enough τ, the linear perturbation will grow too much to retain the linear approximation. This leads to a black hole formation. The important thing is that there is no need to follow this evolution in detail, and we do not focus on the value of the amplitude ϵ where the perturbation becomes nonlinear. We only need to see that the Cauchy data at $\tau = \tau_*$ depend on r through the argument x. Here we obtain

$$Z(x,\tau_*) \simeq Z_*(x) + \epsilon Z_0(x) \tag{2.7}$$

Changing to t, r we get

$$Z(r.t_* - L_*) \simeq Z_*(-\frac{r}{L_*}) + \epsilon Z_0(-\frac{r}{(}L_*),\ L_* \equiv Le^{-\tau *} \tag{2.8}$$

The data at $t = t_*$ depend on the initial data at $t = 0$ of the overall scale L_*. The field equations do not have an intrinsic scale, while the solution at t_* must be universal. In proper coordinates,

such as the polar-radial coordinates chose by Choptuik, it has the form of

$$Z(r,t) = f(\frac{r}{L_*}, \frac{t-t_*}{L_*}), \tag{2.9}$$

where f is some function which is universal for all 1-parameter families [10]. This universality of the solution works for all $t > t_*$, before and after the breaking down of the approximation of linear perturbation around the critical solution. It is obvious that the black hole mass must be proportional to L_*, because it has a length dimension and L_* is the only length scale here. So we know

$$M \propto L_* \propto (p - p*)^{1/\lambda_0} \tag{2.10}$$

Note that the critical exponent satisfies $\lambda = 1/\lambda_0$.

The adjustment of the scaling law in the case of DSS type of critical solution was predicted in [11], and confirmed in simulation works by Hod and Piran [12], claiming that "on the straight line relating $ln\ M$ to $ln(p - p*)$, a periodic "wiggle" or "fine structure" of small amplitude is superimposed":

$$ln\ M = \lambda ln(p - p_*) + c + f[\lambda ln(p - p_*) + c], \tag{2.11}$$

where $f(z) = f(z + \Delta)$. f is a periodic function which is universal with respect to initial data, and the only parameter depends on the family of initial data is c. c presents a shift of the 'wiggly' line in the direction of $ln(p - p_*)$.

It is obvious that for solutions near the critical one, the maximal scalar curvature scales exactly like the black hole mass, with a critical exponent 2γ. It is simpler to "measure the critical exponent and the fine-structure in the subcritical regime from the maximum curvature than from the black hole mass in the supercritical regime"[13].

2.2.4 Scale-invariance and self-similarity

There is often additional symmetries of fixed points in dynamical systems. In the case of type II critical phenomena, the critical point is a spacetime that is self-similar, or scale-invariant. These symmetries can be either discrete or continuous. We describe the continuous symmetry

first because it is simpler. In Newtonian physics, a solution Z is self-similar if it has the form

$$Z(\vec{x},t) = Z[\frac{\vec{x}}{f(t)}] \tag{2.12}$$

We call it self-similarity of the first kind if the function $f(t)$ is derived from dimensional considerations alone. An example of this is $f(t) = \sqrt{\lambda t}$ for the diffusion equation $Z_{,t} = \lambda \delta Z$. If the questions are more complicated, we can get sigular self-similar solution at the limit, where $f(t)$ might include additional dimensionful constants, like $(t/L)^{\alpha}$, where α, namely an anomalous dimension, does not depend on dimensional questions. However it is relavant to the solution of the eigenvalue[14].

A CSS of the spacetime in GR is in correspondence to a homothetic vector field. This relation is of the form

$$L_{\xi} g_{ab} = 2 g_{ab} \tag{2.13}$$

We can treat this as a type of conformal Killing vector, which satisfy that

$$L_{\xi} R^{a}_{bcd} = 0 \tag{2.14}$$

then we have

$$L_{\xi} G_{ab} = 0 \tag{2.15}$$

However, the inverse statement is not true: "The Riemann tensor and the metric need not satisfy 2.13 and 2.14 if the Einstein tensor obeys 2.15".

When it is a perfect fluid matter type, see 2.21, it satisfies 2.13, 2.15 and the Einstein equations that

$$L_{\xi} u^{\alpha} = -u^{\alpha},\ L_{\xi\rho} = -2\rho,\ L_{\xi p} = -2p \tag{2.16}$$

It is similar for a massless scalar field ϕ type of matter, with stress-energy tensor (3.1), it satisfies

$$L_{\xi\phi} = \kappa \tag{2.17}$$

κ here is a constant.

In coordinates $x^\mu = (\tau, x^i)$, the metric coeffiecients are

$$g_{\mu\nu}(\tau, x^i) = e^{-2\tau}\tilde{g_{\mu\nu}}(x^i) \tag{2.18}$$

with τ is the negative logarithm of a spacetime scale, x^i are dimensionless coordinates. In these coordinates, the homothetic vector field is

$$\xi = -\frac{\partial}{\partial\tau} \tag{2.19}$$

In these coordinates, the CSS scalar field is of the form

$$\phi = f(x) + \kappa\tau. \tag{2.20}$$

And the matter type of perfect fluid with stress-energy

$$G_{ab} = 8\pi[(p+\rho)u_a u_b + p g_{ab}] \tag{2.21}$$

gives CSS solutions, where the direction of u^a depends only on x. The density can be written as

$$\rho(x.\tau) = e^{2\tau} f(x) \tag{2.22}$$

Then we see the situation of a DSS in these coordinates. This was carried out in[15]:

$$g_\mu\nu(\tau, x^i) = e^{-2\tau}\tilde{g}_{\mu\nu}(\tau, x^i),\ where\tilde{g}_{\mu\nu}(\tau, x^i) = \tilde{g}_{\mu\nu}(\tau + \Delta, x^i) \tag{2.23}$$

The conformal metric $\tilde{g}_{\mu\nu}$ does now depend on τ. Like the CSS, DSS has a geometric formulation: If there is a discrete diffeomorphism Φ and a real constant Δ, then a spacetime is DSS, as

$$\Phi^* g_{ab} = e^{2\Delta} g_{ab} \tag{2.24}$$

where $\Phi^* g_{ab}$ is the pull-back of g_{ab} under Φ. We see this as a definition of DSS, which is independent of any particular vector field ξ. The Schwarzschild-like coordinates

$$ds^2 = -a^2(r,t)dt^2 + a^2(r,t)dr^2 + r^2 d\Omega^2 \tag{2.25}$$

can be brought into the form 2.23 by a simle transformation of the coordinates. The massless scalar is then of the form

$$\phi = f(\tau, x^i) + \kappa\tau,\ where f(\tau, x^i) = f(\tau + \Delta, x^i) \tag{2.26}$$

with κ a constant.(In the Choptuik critical solution).
We want to emphasize that any coordinates x^i can be introduced on the surface $\tau = 0$, and we may fix the surface by our own interest. In spherical symmetry, τ-surfaces can be chosen to be spacelike in non-global coordinate systems, for example t ¡0. Also, we can find global coordinate systems, where τ-surfaces must become spacelike at large r.

2.3 The scalar field

In this section we plan to review the Einstein field equations and Choptuiks observations at the black hole threshold. Then we look at some recent work on the global structure of Choptuik's critical solution.

2.3.1 Field equations in spherical symmetry

Critical phenomena in gravitational collapse were first discovered in the model of a spherically symmetric, massless scalar field ϕ minimally coupled to general relativity.
We consider a spherically symmetric, massless scalar field minimally coupled to general relativity. The Einstein equations are

$$G_{ab} = 8\pi(\nabla_a\phi\nabla_b\phi - \frac{1}{2}g_{ab}\nabla_c\nabla^c\phi). \tag{2.27}$$

The equation of matter is

$$\nabla_a \nabla^a \phi = 0. \tag{2.28}$$

Choptuik chose Schwarzschild-like coordinates:

$$ds^2 = -\alpha^2(r,t)dt^2 + a^2(r,t)dr^2 + r^2 d\Omega^2 \tag{2.29}$$

where $d\Omega = d\theta^2 + sin^2\theta d\phi^2$ is the metric on the unit 2-sphere. In order to fix the coordinate, Choptuik chose $\alpha = 1$ at $r = 0$, then t is the proper time of a observer in the central. Then we have

$$\Phi = \phi_{,r},\ \Pi = \frac{a}{\alpha}\phi_{,t} \tag{2.30}$$

the wave equation is a first-order system,

$$\Phi_{,t} = (\frac{\alpha}{a}\Pi)_{,r}, \tag{2.31}$$

$$\Pi_{,t} = \frac{1}{r^2}(r^2\frac{\alpha}{a}\Phi)_{,r} \tag{2.32}$$

We find four components of the Einstein equations which are algebraically independent here. One of the components is a linear relevant with the others, so we count it 3. These three contain only first derivatives of the metric, namely $a_{,t}, a_{,r}$, and $\alpha_{,r}$, and are

$$\frac{a_{,r}}{a} + \frac{a^2-1}{2r} = 2\pi r(\Pi^2 + \Phi^2), \tag{2.33}$$

$$\frac{\alpha_{,r}}{\alpha} - \frac{a_{,r}}{a} - \frac{a^2-1}{r} = 0 \tag{2.34}$$

$$\frac{a_{,t}}{\alpha} = 4\pi r\Phi\Pi. \tag{2.35}$$

Because of spherical symmetry, the only dynamics is in the scalar field equations 2.31 3.23

2.3.2 The blackhole threshold

Two functions $\Pi(r,0)$ and $\Phi(r,0)$ gives free data for the system. Choptuik calculated several 1-parameter families of such data by using the data for varied values of the parameter. p is taken to be the amplitude of the Gaussian. For large enough amplitude the scalar field will form a black hole, and for other small amplitude, it will disperse. Choptuik found that "in all 1-parameter families of initial data he investigated he could make arbitrarily small black holes by fine-tuning the parameter p close to the black hole threshold. An important fact is that there is nothing visibly special to the black hole threshold". Close to the black hole threshold, if we do not evolve the given data set for a sufficient long time, it is unreasonable to judge whether it will form a black hole or not. As $p \to p_*$ along the family, the spacetime varies on ever smaller scales. Choptuik was able to determine p_* to a relative precision of 10^{-15}. He made the smallest black holes to be 10^{-6} times the ADM mass. From those smallest black hole masses up to 0.9 of the ADM mass (for some families), which is over six orders of magnitude, the power-law scaling was always applicable. Choptuik therefore assumed that "γ is the same for all 1-parameter families of smooth, asymptotically flat initial data that depend smoothly on the parameter, and that the approximate scaling law holds ever better for arbitrarily small $p \to p_*$".

2.3.3 Global structure of the critical solution

The critical spacetime metric in adapted coordinates can be written as the product of an exponent $e^{2\tau}$ and a regular metric. We can see from this general form that $\tau = \infty$ is a curvature singularity. Ricci and Rieman invariants break like $e^{4\tau}$ at the singularity (unless in the flat spacetime). The Weyl tensor like C^a_{bcd} is conformally invariant. This implies that as $\tau \to \infty$, the components with such index position remain finite. This type of singularity is called "conformally compactifiable" or "isotropic".

[16] has given accurate definition of the global structure of the scalar field critical solution. It is based on the analyticity at the past light-cone of the singularity and at the centre of spherical

symmetry. It is called the self-similarity horizon (SSH). Then they analyze the critical solution singularity at the future light-cone, which is the Cauchy horizon (CH). We may choose global coordinates τ and x, in order to get the SSH, the CH and the regular center $r = 0$ to be linear with respect to constant x. Also the surfaces of constant τ cannot be tangent to those lines of x, which is shown in Figure 2.3.

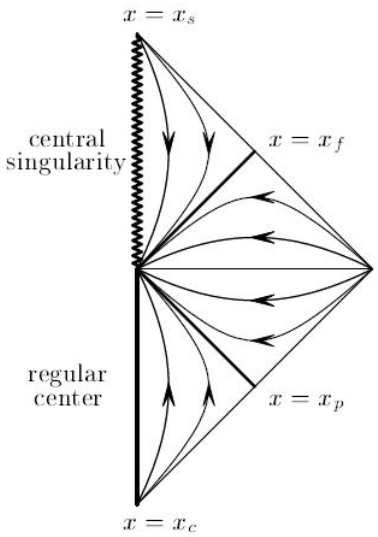

Figure 2.2: The spacetime diagram of all generic DSS continuations of the scalar field critical solution, from [16]. The naked singularity is strong timelike with negative mass. There is a unique continuation where the singularity is replaced by a regular centre except at the spacetime point at the base of the CH, which is still a strong curvature singularity. Cannot have other diagram if the continuation is DSS. The lines with arrows are lines of constant x. The arrow points towards larger curvature in the direction of $\partial/\partial\tau$.

The scalar field will, to approach the CH, oscillates infinite times with the amplitude decaying to zero. The scalar field here is

$$\phi(x,\tau) \simeq F_{reg}(\tau) + \mid x \mid^{\epsilon} F_{sing}[\tau + H(\tau) + Kln \mid x \mid], \tag{2.36}$$

At $x = 0$ we get the SSH. Note here F_{reg}, $F_sing(\tau)$ and $H(\tau)$ are periodic functions whose period is Δ. They have been accurately computed with numerical scheme. When $\epsilon > 0$, the scalar field is continuous but not differentiable with respect to x on the CH. It is also smooth with respect to τ. We see similar conclusion for the curvature and the metric. The ratio m/r (m is the Hawking mass) on the CH, however, is not zero but has a value ordered 10^{-6}. We know that except for the singular point, the CH is regular with smooth data. So it is not obvious

why there are different continuations. We find some explanation in [16], which considered all DSS continuations. In a DSS analysis, the solution on the future side of the CH is similar to Equation 2.36. We have the freedom to choose $F_{sing}(\tau)$ on the future side of the CH, while $F_{reg}(\tau)$ remains the same on both sides. There is one particular $F_{sing}(\tau)$ can give a regular centre on the future side of the CH. Here the naked singularity becomes a point. The numerical result of such continuation showed that it is nearly but not quite Minkowski, with m/r stays small on the future side of the SSH. Other cases of DDS continuations have a "naked, timelike central curvature singularity with negative mass". See the continued solution of DSS spacetime diagram in Figure 2.2.

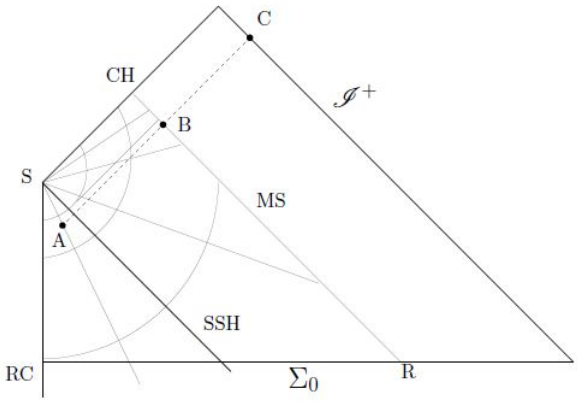

Figure 2.3: As can be seen from the graph above, the conformal diagram which corresponds to the critical solution mathced to an asymptotically flat one (RC: regular centre, S: singularity, SSH: self-similarity horizon). The curved lines show the constant coordinate τ. On the other hand, the conberging straight lines present another constant coordinate x. Assume that the initial data on the cauchy surface CS is the exact critical solution out to the 2-sphere R, continually, we can extend the these data smoothly to some asymptotically flat one, as a result, the future null infinity $\mathscr{I}_+$ does exist. Also, the spacetime is not able to be continued above the Cauchy horizon CH. The redshift between point A and B is finite because of salf-similarity, and for the redshift between B and C is finite because of asymptotic flatness.

2.4 Near the threshold

Choptuiks results suggests: in smooth, generic, asymptotically flat spacetime, "fine-tuning" the initial data to the black hole threshold gives co-dimension one set of data; the time evolution of the critical solution contains at least a point singularity. So the cosmic censorship (see [0] [33] for details) hypothesis must be set as "generic smooth initial data for reasonable matter

do not form naked singularities". Not as much as one naturally expected, Christodoulou [18] proved that the formation of naked singularity is "not generic, but in a rather larger function space, functions of bounded variation"; and in the past light-cone, the instability of the naked singularity he found is not differentiable. Naturally we see in critical collapse, generic smooth initial data can generate the naked singularity. So it is not very clear why the numerical results shows the naked singularities are generic co-dimension one in the space with smooth initial data.

We want to discuss how such "fine-tuning" effect the naked singularities. Firstly, we look at the exact critical solution. Note in the critical solution, α, defined in 2.29, is bounded below and above. So at observers at any two points on a radial null geodesic outwards to the past of CH see a redshift which is bounded below and above. Therefore a higher curvature point can be observed form a lower curvature point, at the exact critical solution.

Secondly, we consider a spacetime where the critical solution in the centre can be matched smoothly to a asymptotically flat space outside. Here the flat spacetime covers part of the critical solution including the singularity, see Figure 2.2.

Next, we look at the fine-tunning to the black hole threshold of the asymptotically flat initial data. The approximation of such spacetimes can be found in 2.5. We see as the data approaching the singularity and the approximation becoming better, most of the perturbations decay, until a significantly growing perturbation occurs. (The growing on is claimed to be due to the fine-running starts small.) Then we approach a highest curvature with the scale of

$$R_{max} \propto (p - p_*)^{2\gamma}, \tag{2.37}$$

which can still be seen from $\mathscr{I}^+$.

Finally, we consider the perfect fine-tuning limit. Here we no longer see a growing perturbation, but all others still decay as we reach the naked singularity. We observe from 2.5 that this is true no matter in which direction (spacelike, past, or future) the singularity is reached.

Chapter 3

Gravititional Collapse in Anti de sitter spacetime

3.1 Overview

We have pointed out the significance of studying AdS collaspe in chapter 1 and we have reviewed the critical phenomena observed in flat space black hole formation in chapter 2. Logically, we think about studying the threshold of AdS black hole formation to see what kind of critical behavior is applied. Pretorius and Choptuik gave numerical simulations of the formation of black holes from the gravitational collapse of a massless, minimally-coupled scalar field in 2+1 dimensional AdS spacetime, and found a continuously self-similar solution and corresponding mass-scaling exponent of approximately 1.2[22].

As we mentioned, in an isolated flat space system, large enough initial amplitudes lead to black hole fromation while others lead to complete dispersion of the mass-energy to infinity. AdS spacetime is different from flat Minkowski space, which is know to be stable under weakly perturbation. What shows its difference from flat or de-Sitter spacetimes, is the existence of a timelike boundary at (spatial and null) infinity [20]. Bizoń and Rostworowski's results [21] suggest that "AdS space is unstable under arbitrarily small generic perturbations". Any initial amplitude did not form a black hole in the first place will reflect off the boundary of AdS and

increase a bit by each reflection(see section 3.3). After several times of reflection, the amplitudes will finally reach the threshold and lead to the formation of a black hole.

In this chapter, we will study the gravititional collapse in an example of 2+1 dimensional AdS first and focus primarily on the threshold for black hole formation (Critical AdS collapse 3.2). Then we want to discuss the formation of a black hole with arbitrarily small initial amplitude reflecting off the AdS boundary enough times (here we categorized as non-critical AdS blackhole formation 3.3).

3.2 Critical AdS collapse

We present Pretorius and Choptuik's results of a numerical study of the collapse and formation of vacuum black holes from a massless scalar field in $2+1d$ AdS. Here we want to give some conclusions on critical behaviour of AdS collapse rather than present the numerical data itself. We are intersted in whether we can observe critical phenomena at the black hole threshold, similar to what we mentioned in last chapter. If we tune the initial data carefully, can we obtain a solution which is universal with respect to the initial data? The result shows that the system have a CSS solution in the critical limit, with a scaling exponent $\gamma = 1.20.05$[22].

3.2.1 Coordinates and numerical scheme

The following calculation shows Pretorius and Choptuik's choice of coordinate system. First, we solve the Einstein field equation in 3 spacetime dimensions with cosmological constant $\Lambda \equiv -1/l^2$, coupled to a massless Klein-Gordon(KG) field

$$R_{ab} - \frac{1}{2}Rg_{ab} + \Lambda g_{ab} = \kappa T_{ab} \tag{3.1}$$

where the stress-energy tensor for the KG field ϕ is

$$T_{ab} = \phi_{;a}\phi_{;b} - \frac{1}{2}g_{ab}\phi_{;c}\phi^{;c} \tag{3.2}$$

In the case of simplest symmetric of a minimally-coupled scalar field here, so ϕ satisfies the wave equation

$$\Box\phi = \phi^{a}_{;a} = 0 \tag{3.3}$$

Considering the causal structure of AdS spacetime and the boundary conditions on the field ϕ, (for more details, see[22]), the coordinate system is chosen to be the form

$$ds^2 = \frac{e^{2A(r,t)}}{cos^2(r/l)}(dr^2 - dt^2) + l^2 tan^2(r/l) e^{2B(r,t)} d\theta^2. \tag{3.4}$$

$A(r,t)$ and $B(r,t)$ are functions of (r,t). It is easy to notice when $A = B = 0$ the above metric is exactly AdS spacetime. In this metric, we also note radial null geodesics has a speed $dr/dt = \pm 1$ of coordinates, which is constant. Null infinity $\mathscr{I}$ is at $r = \pi l/2$. The metric has singularity at $\mathscr{I}$. Boundary conditions can be set on A and B to obtain asymptotically AdS spacetime. For the non-rotating collapse, θ has no dynamical significance. Defining

$$\Phi(r,t) = \phi_{,r},\ \Pi(r,t) = \phi_{,t} \tag{3.5}$$

and using units where $\kappa = 4\pi$. Expand 3.1 3.2 3.3, we obtain these equations with the metric:

$$A_{,rr} - A_{,tt} + \frac{1 - e^{2A}}{l^2 cos^2(r/l)} + 2\pi(\Phi^2 - \Pi^2) = 0, \tag{3.6}$$

$$B_{,rr} - B_{,tt} + B_{,r}(B_{,r} + \frac{2}{l cos(r/l) sin(r/l)}) - (B_{,t})^2 + \frac{2(1 - e^{2A})}{l^2 cos(r/l)} = 0, \tag{3.7}$$

$$B_{,rr} + B_{,r}(B_{,r} - A_{,r} + \frac{1 + cos^2(r/l)}{l cos(r/l) sin(r/l)}) - \frac{A_{,r}}{l cos(r/l) sin(r/l)} - A_{,t}B_{,t} + \frac{1 - e^2 A}{l^2 cos^2 r/l} + 2\pi(\Phi^2 + \Pi^2) = 0, \tag{3.8}$$

$$B_{,rt} + B_{,t}(B_{,r} - A_{,r} + \frac{cot(r/l)}{l}) - A_{,t}(B_{,r} + \frac{1}{l sin(r/l) cos(r/l)}) + 4\pi\Phi\Pi = 0 \tag{3.9}$$

and

$$[tan(r/l)e^B\Phi]_{,r} - tan(r/l)[e^B\Pi]_t = 0. \tag{3.10}$$

In 3+1d, equations 3.8 and 3.9 are the Hamiltonian and momentum constraints respectively, while equations 3.6 3.7 are combinations of the evolution and constraint equations. 3.10 is the wave equation of the scalar field. There are two unknown geometric variables$A(r,t)$ and $B(r,t)$; hence one needs to use at least two of the four equations [3.6-3.9]. In [21], ther chose to use 3.6 and 3.7 to evaluate A and B. And [3.8] and [3.9] can be used to estimate errors. With respect to initial conditions, they choose to specify $\Phi(r,0)$ and $\Pi(r,0)$. The Ricci scalar of this spacetime is

$$R = \frac{4\pi cos(r/l)^2}{e^{2A}l^2}(\Phi^2 - \Pi^2) - \frac{6}{l^2} \tag{3.11}$$

The Weyl tensor is zero. Other non-zero curvatures can be written as polynomial expression of R.

Regular conditions

We regular $A(r,t), B(r,t), \Phi(r,t)$ and $\Pi(r,t)$ at the origin, r = 0, and at I, $r = \pi l/2$. We have the following five conditions at r = 0,

$$A_{,t}(0,t) = B_{,t}(0,t) \tag{3.12}$$

$$A_{,r}(0,t) = 0 \tag{3.13}$$

$$B_{,r}(0,t) = 0 \tag{3.14}$$

$$\Phi(0,t) = 0 \tag{3.15}$$

$$\Pi_{,r}(0,t) = 0 \tag{3.16}$$

and at $r = \pi l/2$

$$A(\pi l/2,t) = A, r(\pi l/2,t) = A_{,r}(\pi l/2,t) = 0 \tag{3.17}$$

$$B_{,r}(\pi l/2,t) = 0 \tag{3.18}$$

$$\Phi(\pi l/2, t) = 0 \tag{3.19}$$

$$\Pi(\pi l/2, t) = 0. \tag{3.20}$$

Initial conditions

We have the freedom to choose the scalar field $\Phi(r, 0)$ and $\Pi(r, 0)$, the metric $B(r, 0)$ and its time derivative $B_{,t}(r, 0)$ for initial conditions at $t = 0$. Then they numerically solve for $A(r, 0)$ and $A_{,t}(r, 0)$ by inserting the hamiltonian and momentum constraints 3.8 and 3.9. To be simple they set $B(r, 0) = B_{,t}(r, 0) = 0$. We take a gaussian curve to the n-th power for the initial scalar field $\phi(r, 0)$,

$$\phi(r, 0) = Pe^{((r-r_0)/\sigma)^{2n}}, \tag{3.21}$$

and a family of harmonic functions

$$\phi(r, 0) = Pcos^2(rn/l), \tag{3.22}$$

where P, r_0, σ and n are constants. They also set $\Pi(r, 0) = \Phi(r, 0), \Pi(r, 0) = \Phi(r, 0)$ or $\Pi(r, 0) = 0$ respectively.

Numerical Scheme

To solve the set of equations 3.63.7 and 3.10, Pretorius1 and Choptuik converted them to "a system of finite difference equations on a uniform coordinate grid using a two-time level Crank-Nicholson scheme". They also add Kreiss-Oliger style dissipation [25] to control high-frequency solution components, which is important to keep the method stable.
To detect black holes and excising sigularities, they implemented *singularityexcision*, a technique motivated by the *black hole excision* strategy, which was suggested by Unruh.

3.2.2 Results

After following Pretorius and Choptuiks work, we study black hole formation from the collapse of a minimally-coupled massless scalar field in 2+1 dimensional AdS spacetime, and now we can draw some conclusions according to the numerical results.

Outside of the event horizon the spacetime settles down to a BTZ form; in the interior a central, spacelike curvature singularity develops. At the threshold of black hole formation we discovered that the scalar field and spacetime geometry evolve towards a universal, CSS form of solution. When a point particle is present at the origin the critical solution is shifted in central proper time by an amount with respect to the mass of the particle. Through examining the behavior of the curvature scalar during sub-critical evolution, its deduced that the universal scaling exponent γ for this system is roughly 1.2 ± 0.05. We have to admit that this value differs from the scaling exponent $1/2$ computed by Peleg and Steif [23] for the collapse of thin rings of dust and by Birmingham and Sen [24] for particle collisions. On the other hand, those works took other forms of matter into consideration, and the phase transition was between black hole and naked singularity formation. Thus one would not expect to see the same exponent here.

In the end of [22], they also proposed a question asking if any small initial data in AdS will form a black hole eventually if one waits long enough, regarding the properties of AdS boudary. We will discuss the relevant work was carried out by Bizoń and Rostworowski[21] in next section.

3.3 Non-critical AdS black hole formation

In this section, we want to know what will happen to arbitrarily small amplitude in AdS spacetime, which does not lead to a black hole formation in the first place. We discuss this by looking at nonlinear evolution of a weakly perturbed AdS apace. The results of four-dimensional AdS spherically symmetric Einstein massless scalar field equations, carried our by Bizoǹ and Rostworowski[21], shows that AdS space is unstable under arbitrarily turbulent. Which implies no matter how small the initial amplitude is there will always be a collapse and black hole formation if one waits long enough. We also discussed in section 3.3.2 if this is true for any

d+1 dimensional AdS ($d \geq 3$).

3.3.1 Weak turbulence and AdS instability

For an asymptotically AdS apacetime, there is a timelike boundary at (spatial and null) infinity which plays a role like the wall of a closed box. We obtain a Hamiltonian consevative system ,for no-flux boundary conditions, where energy cannot escape the boundary. Therefore we will see unstability of AdS space, as shown below, when applying the KAM theory for partial differential equations.

The Model

The model used in [21] is a self-gravitating spherically symmetric real massless scalar field in $3 + 1$ dimensional asymptotically AdS. The Einstein-scalar system with negative cosmological constant Λ is of the form

$$G_{\alpha\beta} + \Lambda g_{\alpha\beta} = 8\pi G(\partial_\alpha\phi\partial_\beta\phi - \frac{1}{2}g_{\alpha\beta}(\partial\phi)^2), \tag{3.23}$$

$$g^{\alpha\beta}\nabla_\alpha\nabla_\beta\phi = 0. \tag{3.24}$$

For the metric we assume the ansatz

$$ds^2 = \frac{l^2}{cos^2x}(-Ae^{-2\delta}dt^2 + A^{-1}dx^2 + sin^2x d\Omega^2), \tag{3.25}$$

where $l^2 = -3/\Lambda$ and $d\Omega^2$ is the metric on the round unit two-sphere. Assume that A, δ, and ϕ We introduce auxiliary variable $\Phi = \phi'$ and $\Pi = A^-1e^\delta\phi$, and insert 3.25 into 3.23 3.24, we get a coupled quasilinear elliptic-hyperbolic system. The wave equation here is of the form

$$\dot{\Phi} = (Ae^{-\delta}\Pi)',\ \dot{\Pi} = \frac{1}{tan^2x}(tan^2xAe^{-\delta}\Phi), \tag{3.26}$$

and the constraints (regarding units $4\pi G = 1$)

$$A' = \frac{1 + 2sin^2x}{sinxcosx}(1 - A) - sinxcosxA(\Phi^2 + \Pi^2), \tag{3.27}$$

$$\delta' = -sinxcosx(\Phi^2 + \Pi^2). \tag{3.28}$$

The pure AdS solution is given by $\phi = 0, A = 1, \delta = 0$, and the length scale l drops out from the equations. We want to solve the equations [3.26]-[3.28] for smooth initial data with finite total mass. To obtain smoothness near $x = 0$, we get the power series expasions

$$\phi(t, x) = f_0(t) + \mathcal{O}(x^2),\ \delta(t, x) = \mathcal{O}(x^2),\ A(t, x) = 1 + \mathcal{O}(x^2), \tag{3.29}$$

normalization $\delta(t, 0) = 0$ is used here. Thus, t is the proper time observed in the centre. Since the total mass M is finite and consider the smoothness at spatial infinity, we obtain that near $x = \pi/2$ there must be $\rho = \pi/2 - x$.

$$\phi(t, x) = f_\infty(t)\rho^3 + \mathcal{O}(\rho^5),\ \delta(t, x) = \delta_\infty + \rho,\ A(t, x) = 1 - 2M\rho^3 + \mathcal{O}(\rho^6), \tag{3.30}$$

where M and free function $f_\infty(t), \delta(t, x)$ determine the power series expasions uniquely. There is no need to specify boundary conditions at infinity for smooth initial data, because we do not have freedom to impose the boudary data, wich means it is natrually defined (see[26] for proof).

Numerical results

The numerical scheme in [21] is to solve the above system with fourth-order accurate finite-difference code by using the method of lines and a 4th-order RungeKutta scheme to integrate the wave equation in time. At each step the metric functions were updated by solving the hamiltonian constraint 3.27 and the slicing condition 3.28.

Solutions shown in Figure 3.1 and Figure 3.2 were generated from Gaussian-type initial data

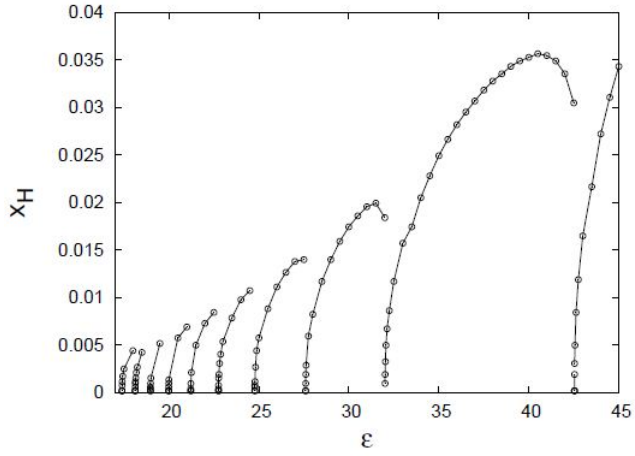

Figure 3.1: [21] Horizon radius vs amplitude for initial data (9). The number of reflections off the AdS boundary before collapse varies from zero to nine (from right to left). $x_H(\epsilon)$ has the shape of the right continuous sawtooth curve with finite jumps at each ϵ_n.

of the form

$$\Phi(0,x) = 0,\ \Pi(0,x) = \frac{2\epsilon}{\pi} exp(-\frac{4tan^2 x}{\pi^2\sigma^2}), \tag{3.31}$$

with varying amplitude ϵ and fixed width $\sigma = 1/16$. For large enough amplitudes we see quick collapses. There is an horizon at x_H where $A(t,x)$ is zero. This is the sign for a collapse. When the amplitude go smaller, the horizon radius x_H also become smaller and goes to zero for some critical amplitude ϵ_0. The critical behaviour is generally the same as in flat space described in last chapter. In critical behaviour here, nothing depends on the Λ constant, so the solution with critical amplitude ϵ_0 is just the DSS solution discovered by Choptuik in the corresponding dimensions in flat space. For smaller amplitudes that very close to ϵ_0 the wave moves to infinity, reflects off the boundary, and collapses as soon as arriving the center. By slowly lowering the amplitude we observe the 2nd critical value ϵ_1 with $x_H = 0$. As gradually lowering ϵ, this process repeats, and we always obtain Choptuiks solution in the $n-th$ time the wave is at the center.

Then we look at the updating of general small initial data, focusing on early and intermediate pre-collapse phases of the process. The Ricci scalar at the centre, $R(t,0) = -2\Pi^2(t,0)/l^2 - 12/l^2$, can be a indicator for instability. An upper envelope of these oscillations is shown in Figure 3.2a, where we can tell every phase of the evolution. During the first phase the amplitude remains nearly constant but after a while a 2nd phase which looks like exponential growth started,

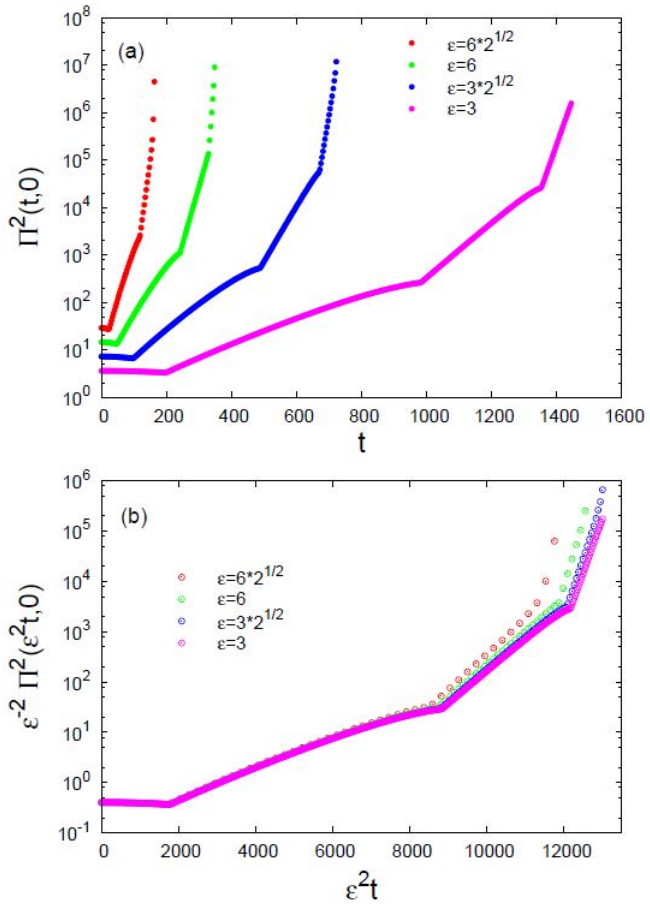

Figure 3.2: [21] (a) $\Pi 2(t,0)$ for solutions with initial data for four moderately small amplitudes. For clarity of the plot only the upper envelopes of rapid oscillations are depicted. After making between about fifty (for $\epsilon = 6\sqrt{2}$) and five-hundred (for $\epsilon = 3$) reflections, all solutions finally collapse. (b) The curves from the plot (a) after rescaling.

followed by a 3rd phases of sharper growth. And eventually it collapses. It is seen that the time of the second phase scales as $\epsilon 2$ (see Figure 3.2b), which implies that small perturbations begin to grow at this point. This behaviour demonstrates the instability of AdS space.

Bizoń and Rostworowski tried to explain the reason of above observation. They classified data into two kinds - non-resonant (one-moda) data and resonant (two-mode) data. For non-resonant mode the solution is always close to the initial data during the entire evolution. This indicates stability. On the contray, for resonant mode we see an exponential instability with time $t = \mathcal{O}(\epsilon - 2)$.

They reached a agreement that such instability of AdS is triggered by a resonant mode mixing which "gives rise to diffusion of energy from low to high frequencies", which is still a conjecture and not yet been proven.

More evidence shows that such observation of weak turbulence is applicable for different bounded domain nonlinear wave equations. Recently it has been proven for the nonlinear Schrö dinger equation on torus [27]. The results in [21] presented above, however, is advanced in the direction of Einstein equations.

3.3.2 AdS collapse in higher dimensions

We have known that AdS is unstable against gravitational collapse in 3+1 dimensional, but is this also true for higher dimension cases where $d \geq 3$. Jalmuzna, Rostworowski and Bizon indicated in[27] that the weakly turbulent instability of all higher dimensional (d+1 for $d \geq 3$) AdS is true and corrected the contrary claim made in [28]. They used very similar model and numerial method as in [21], just ajusted the equations to d+1 dimensions. So we present the numerical result in Figure 3.3 without listing all the equations here.

We can draw similar conclusion as the 4 dimensional case shown in 3.3.1. Numerical results shows that for small enough ϵ in this scaling continues almost all the way to the collapse, which is $t_H(\epsilon) \sim \epsilon 2$. The evidence for this fact is shown in Figure 3.3 which depicts the evolution of three solutions with small amplitudes differing by a factor of $\sqrt{2}$.

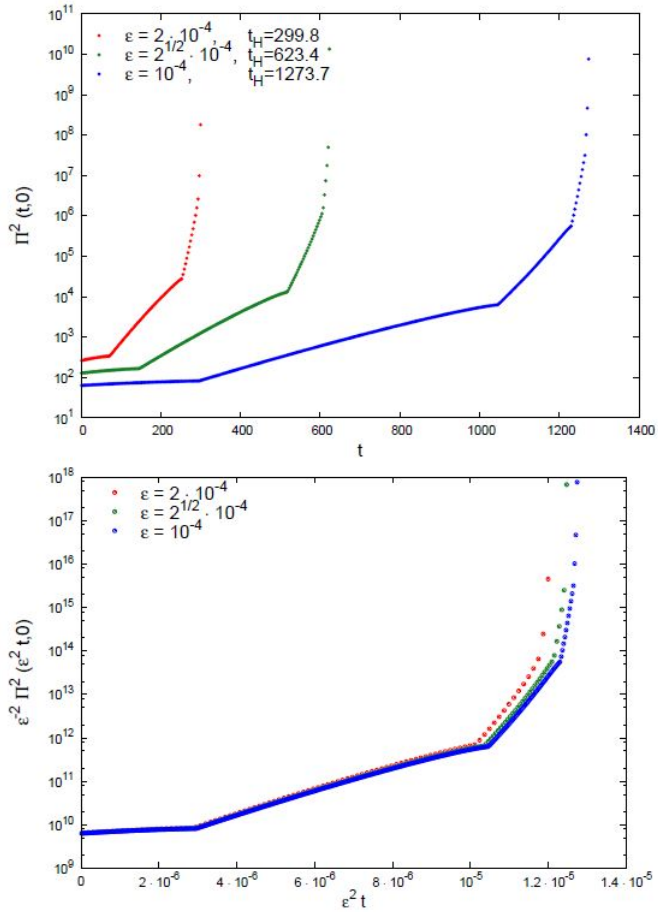

Figure 3.3: [27] Upper plot: the upper envelope of $\Pi^2(t,0)$ for initial data with three relatively small amplitudes. After making 95 (for $\epsilon = 0.0002$), 198 (for $\epsilon = \sqrt{2} \times 0.0001$, and 405 (for $\epsilon = 0.0001$) reflections, all solutions eventually collapse. Lower plot: the curves from the upper plot after rescaling $\epsilon^{-2}\Pi^2(\epsilon^2 t, 0)$ seem to converge to a limiting curve.

Chapter 4

Conclusion

In this thesis, we reviewed "critical phenomena" in gravitational collapse both in asymptotically flat space 2 and Anti de-Sitter spacetime 3. We see samilar critical behaviour and self-similar solutions at the black hole threshold. This gives support to the statement "Critical phenomena give a natural route from smooth initial data to arbitrarily large curvatures visible from infinity, and are therefore likely to be relevant for cosmic censorship, quantum gravity, astrophysics, and our general understanding of the dynamics of general relativity." in [31]. In the last two sections of Chapter 3, we discussed the non-critical cases of AdS black hole formation based on numerical work of [21] and [27]. We see an interesting conclusion that in asymptotically AdS_{d+1} ($d \geq 3$), any initial amplitude did not form a black hole in the first place will reflect off the boundary of AdS and increase a bit by each reflection and finally leads to a formation a black hole. In [21], such instability of AdS is claimed to be triggered by "a resonant mode mixing which gives rise to diffusion of energy from low to high frequencies".

One well-known example of AdS/CFT is $AdS_5 \times S^5/N = 4$ Super Yang Mills correspondence (see [32] for details). It will be logical to discuss further what implication might the weakly turbulent instability of AdS_5 give to $N = 4$ Super Yang Mills theory.

Another interesting question is whether the negative cosmological constant Λ is relavent to the observation in the evolution. Is it a decisive factor to triggering a non-critical gravitational collapse in a corresponding spacetime? It will be interesting to carry out further study on this question.

Bibliography

[1] M. Bañados, C. Teitelboim and J. Zanelli, Phys. Rev. Lett. 69, 1849 (1992).

[2] J. M. Maldacena, Adv. Theor. Math. Phys. 2, 231 (1998). hep-th/9711200.

[3] J. Maldacena, "The gauge/gravity duality",(2011). arXiv:1106.6073 [hep-th].

[4] M.W. Choptuik, "Universality and scaling in gravitational collapse of a massless scalar field", Phys. Rev. Lett., 70, 912, (1993).

[5] A.M. Abrahams, and C.R. Evans, "Critical behavior and scaling in vacuum axisymmetric gravitational collaps", Phys. Rev. Lett., 70, 29802983, (1993).

[6] P.R. Brady, C.M. Chambers, and S.M.C.V, Goncalves, ,"Phases of massive scalar field collapse", Phys. Rev. D, 56, R6057-R6061, (1997).

[7] C.R. Evans, and C.S. Coleman, "Critical phenomena and self-similarity in the gravitational collapse of radiation fluid", Phys. Rev. Lett., 72, 1782, (1994).

[8] T. Koike, T. Hara, and S., Adachi, "Critical behaviour in gravitational collapse of radiation fluid - A renormalization group (linear perturbation) analysis", Phys. Rev. Lett., 74, 5170, (1995).

[9] D. Maison, "Non-universality of critical behaviour in spherically symmetric gravitational collapse", Phys. Lett. B, 366, 82, (1996).

[10] E.W. Hirschmann, and D.M. Eardley, "Critical exponents and stability at the black hole threshold for a complex scalar field", Phys. Rev. D, 52, (1995).

[11] c. Gundlach, "Understanding critical collapse of a scalar field", Phys. Rev. D, 55, 695, (1997).

[12] S. Hod, and T. Piran, "Fine-structure of Choptuik's mass-scaling relation", Phys. Rev. D, 55, 440, (1997).

[13] D. Garfinkel, and G.C. Duncan, "Scaling of curvature in sub-critical gravitational collapse", Phys. Rev. D, 58, 064024, (1998).

[14] G.I. Barenblatt, Similarity, Self-Similarity and Intermediate Asymptotics, (Plenum Press, New York and London, 1979).

[15] C. Gundlach, "Understanding critical collapse of a scalar field", Phys. Rev. D, 55, 695, (1997).

[16] J.M. Martn-Garca, and C, Gundlach, Global structure of Choptuiks critical solution in scalar field collapse, Phys. Rev. D, 68, 024011, 125, (2003).

[17] B.J. Carr, and C. Gundlach, Spacetime structure of self-similar spherically symmetric perfect fluid solutions, Phys. Rev. D, 67, 024035, 113, (2003).

[18] D. Christodoulou, The Instability of Naked Singularities in the Gravitational Collapse of a Scalar Field, Ann. Math. (2), 149, 183217, (1999).

[19] D. Garfinkle, and G.C. Duncan, Scaling of curvature in subcritical gravitational collapse, Phys. Rev. D, 58, 064024, 14, (1998).

[20] H. Friedrich, J. Geom. Phys. 17, 125 (1995)

[21] P. Bizon and A. Rostworowski, "On weakly turbulent instability of anti-de Sitter space," Phys. Rev. Lett. 107 (2011) 031102 [arXiv:1104.3702 [gr-qc]].

[22] F. Pretorius and M. W., Choptuik, "Gravitational collapse in (2+1)-dimensional AdS space-time," Phys. Rev. D **62** (2000) 124012 [gr-qc/0007008].

[23] Y. Peleg and A. R. Steif, Phys. Rev. D51, 3992 (1995)

[24] H. Matschull, Class. Quant. Grav. 16, 1069 (1999), D. Birmingham and S. Sen, Phys.Rev.Lett. 84, 1074 (2000), hep-th/9908150

[25] H. Kreiss and J. Oliger, Methods for the Approximate Solution of Time Dependent Problems, Global Atmospheric Research Programme, Publications Series No. 10. (1973)

[26] G. Holzegel and J. Smulevici, arXiv:1103.0712.

[27] J. Jalmuzna, A. Rostworowski and P. Bizon, "A Comment on AdS collapse of a scalar field in higher dimensions," Phys. Rev. D **84** (2011) 085021 [arXiv:1108.4539 [gr-qc]].

[28] D. Garfinkle and L.A. Pando Zayas, arXiv:1106.2339.

[29] S. S. Gubser, I. R. Klebanov, A. M. Polyakov, Phys. Lett. B428, 105-114 (1998). [hep-th/9802109].

[30] E. Witten, Adv. Theor. Math. Phys. 2, 253-291 (1998). [hep-th/9802150].

[31] C. Gundlach and J. M. Martn-Garca, "Critical Phenomena in Gravitational Collapse", Living Rev. Relativity 10, (2007).

[32] O. Aharony, S. S. Gubser, J. M. Maldacena, H. Ooguri and Y. Oz, Phys. Rept. 323 (2000) 183 [hep-th/9905111].

[33] R.M. Wald, "Gravitational Collapse and Cosmic Censorship(1997). [grqc/ 9710068].